![QUIETDRONES 2024 MANCHESTER 8th - 11th September 2024]

A Synthesis Method to Auralize Rotor Noise During Transitional Flight
Session: Auralisation and Acoustic Simulation

Siddhartha Krishnamurthy, NASA Langley Research Center, USA,
siddhartha.krishnamurthy@nasa.gov

Brian C. Tuttle, Analytical Mechanics Associates, USA,
brian.c.tuttle@nasa.gov

Aric R. Aumann, Analytical Services and Materials, USA,
aric.r.aumann@nasa.gov

Stephen A. Rizzi, NASA Langley Research Center, USA,
s.a.rizzi@nasa.gov

Leonard V. Lopes, NASA Langley Research Center, USA,
leonard.v.lopes@nasa.gov

Stefan J. Letica, NASA Langley Research Center, USA,
stefan.j.letica@nasa.gov

D. Douglas Boyd, Jr., NASA Langley Research Center, USA,
d.d.boyd@nasa.gov

Abstract This paper describes new approaches to synthesize Urban Air Mobility (UAM) vehicle rotor/propeller loading and thickness noise and broadband self noise for transitional flight auralization. A vehicle smoothly transitioning between flight states is approximated here as transitioning in time through a series of trimmed steady-state flight conditions. To generate information that helps synthesize loading and thickness noise for transitional flight, this paper describes the development of a tool that combines blade loading, motion, and geometry data from a series of separate trimmed flight states. This paper also describes a method to combine broadband self noise acoustic predictions, each representing a separate trimmed flight state, to synthesize broadband self noise for transitional flight. Different flight profiles of the six-passenger NASA UAM Quadrotor reference vehicle demonstrate these approaches, with each profile specified by a series of trimmed flight states.

Keywords: Auralization, Auralisation, Broadband Noise, Self Noise, Loading Thickness Noise, Synthesis, Transitional Flight, Rotorcraft, Urban Air Mobility, Advanced Air Mobility, NASA Auralization Framework

1. INTRODUCTION

This paper describes new approaches to synthesize rotor/propeller noise for transitional flight auralization. Auralization is a technique for creating audible sound files from numerical data [1]. Numerical data are acoustic predictions that may be in the frequency-domain, time-domain, or both, but the predictions may be missing information for which providing additional inputs and processing, i.e., synthesis steps, are necessary to generate audible sound. Here, auralization refers to the combined process of source noise synthesis, propagation to a ground observer, and receiver simulation [2]. Hence, the synthesis approaches described here refer to creating audible sound files without the propagation and receiver simulation steps.

Transitional flight refers to a rotor/propeller-driven aircraft flying between different flight conditions. A single flight condition occurs when a vehicle is in a trimmed state, i.e., steady flight, such as a level cruise flight condition or a climb flight condition with a constant climb angle. The transitional flight sound synthesis methods discussed in this paper may be used between arbitrary flight conditions. Nevertheless, the fidelity of the transitional flight sound will generally improve if the two consecutive flight conditions are similar. An example of similar flight conditions for transitional flight are climb flight conditions at the same airspeed but different climb angles, e.g., five degrees and 10 degrees.

Auralizations with rotor/propeller transitional flight are intended to be used in human subject tests to assess the noise impact of air vehicles. This is particularly important for future air vehicles, including Urban Air Mobility (UAM) vehicles, for which flight recordings are not available [3]. These future air vehicles are likely to depart and arrive in closer proximity to communities than traditional aircraft, and transitional flight will be part of the departure and arrival maneuvers. Studying the human response to transitioning flight phases through controlled laboratory testing with auralized sounds can inform vehicle design and subsequent in-field community noise testing.

Rotor/propeller noise can come from harmonic and non-harmonic sources [4]. Harmonic noise sources are deterministic, with loading and thickness noise being a prominent harmonic noise source. Non-harmonic noise sources are non-deterministic and include broadband self noise [5]. The auralizations presented in this paper synthesize audible loading and thickness noise and audible broadband self noise for simulated transitional rotor/propeller flight.

There are challenges associated with obtaining the vehicle state data needed to synthesize rotor/propeller noise during transitional flight. Such state data include rotor/propeller aerodynamics and blade deflections, since coupling between the aerodynamic loads and blade structure are important to capture. A flight simulation framework described in Ref. [6] can generate the aerodynamic data needed for sound synthesis for transitional flight, however the framework targeted a real time application which may limit its fidelity. Another potential source for the aerodynamic and blade data is the Fundamental Rotorcraft Acoustic Modeling from Experiments (FRAME) [7] which supplies blade geometry and aerodynamics data using a semi-empirical approach. However, the semi-empirical FRAME approach is currently limited to conventional helicopters. Although computational methods could be used to generate state information for steady-state flight, the computational burden is currently excessive for rotor/propeller aerodynamics and geometry information for a full transitional flight. Medium to high fidelity computational tools can be used to generate separate data for each trimmed state, and additional processing can then be done to combine the separate data to represent transitional flight. Methods described in this paper perform this additional processing to synthesize UAM rotor/propeller sounds for transitional flight of higher fidelity than those that can be produced in real-time.

One tool that offers rotor blade data for individual trimmed states at sufficient fidelity is the second generation Comprehensive Analytical Model of Rotorcraft Aerodynamics and Dynamics (CAMRAD II) [8]. These CAMRAD II data can be used as input to the NASA Aircraft Noise Prediction Program 2 (ANOPP2) [9] to generate acoustic predictions. Innovations described in this paper are used to post-process ANOPP2 acoustic predictions from separate trimmed states into a form amenable to transitional flight sound synthesis. This synthesis is implemented in the NASA Auralization Framework (NAF) [10], a suite of software tools for auralization.

1.1 Paper Contributions

This paper develops methods to auralize UAM vehicles in transitional flight. Two methods are described here: one for loading and thickness noise and the other for self noise. The methods approximate transitional flight as a series of trimmed states with the vehicle transitioning from one trimmed state to another over time. This approximation approach is useful when the aerodynamic and blade data are available for separate trimmed states, such as would be generated using CAMRAD II. Based on this approximation, the following approaches were developed to auralize UAM vehicles in transitional flight:

1. Combine rotor/propeller aerodynamics and geometry data from a series of separate trimmed flight states into a single data structure that enables loading and thickness noise synthesis for transitional flight. This approach is discussed in Section 2.

2. Combine broadband self noise acoustic predictions, each representing a separate trimmed flight state, to synthesize broadband self noise for transitional flight. This approach is discussed in Section 3.

Section 4 explains how these approaches are tested using a single rotor and without applying propagation effects to the synthesized sounds. Section 5 exercises transitional flight sound synthesis to auralize sound for a multi-rotor UAM aircraft, including propagation effects.

2. Loading and Thickness Noise for Transitional Flight

2.1 Existing Loading and Thickness Noise Synthesis Methods

The NAF can synthesize rotor blade loading and thickness noise for auralization. For brevity, the loading and thickness noise will be referred to as tonal noise in the remainder of the paper.

The NAF has two methods to generate tonal rotor noise: additive synthesis and the Formulation 1A (F1A) [11] Synthesis Plugin. The additive synthesis method is intended for generating periodic signals based on existing acoustic predictions of simple harmonic series, and hence is not suitable for arbitrary flight maneuvers. The F1A Synthesis Plugin can synthesize tonal noise for arbitrary flight maneuvers involving unsteady flight with accelerations [12]. This plugin computes the F1A solution to a wave equation for moving surfaces (see Ref. [11] for additional details). The F1A Synthesis Plugin works in three general steps: 1. read blade loading, blade motion, and blade geometry data from a computer file, 2. use the blade data with ANOPP2 functions to predict tonal noise using the F1A approach, 3. post-process the tonal noise prediction into sounds that can be heard over audio devices [13].

In Ref. [14], the F1A Synthesis approach was used to auralize a Bell 206 helicopter main rotor with a flight trajectory involving accelerations and attitude changes. Blade geometry and aerodynamic data were determined using FRAME [7]. No further processing was required on the FRAME-generated data. The semi-empirical data required by FRAME was obtained from flight measurements of the Bell 206 helicopter.

In Ref. [15], the F1A Synthesis Plugin was used to synthesize tonal noise for the NASA UAM Quadrotor Reference vehicle. The flight condition was level cruise at 90 Knots True Airspeed (KTAS). Semi-empirical aerodynamics and geometry data do not exist for the UAM Quadrotor Reference vehicle. Therefore, CAMRAD II supplied the blade loading, motion, and geometry data for the steady flight condition. Although CAMRAD II data exist for other Quadrotor flight conditions, the data will need preprocessing into a form that reflects transitional flight to auralize the Quadrotor with changing flight conditions. The preprocessing step developed for this paper is described in the next section (Section 2.2).

2.2   Combining Rotor Data from Multiple Trimmed States

A newly developed ANOPP2 tool, called the ANOPP2 Series of Periodic to Aperiodic Interpolated Data (ASPAID), interpolates between blade loading, motion, and geometry data from separate trimmed states to approximate state data during transitional flight. CAMRAD II is one tool that can generate the data for the separate states, but other tools can be used if they conform to the ASPAID input format. ASPAID was exercised using CAMRAD II data to produce the results in this paper.

ASPAID makes the following three assumptions:

1. Between any two flight states, the time scale of the transition is large relative to the rotor rotation period.

2. Rotor rotation speeds are constant through the entire flight over all trimmed states.

3. Transition can be represented by a linear interpolation of rotor blade aerodynamics and geometry quantities between trimmed states.

Input for ASPAID are periodic blade data files, such as those from CAMRAD II, corresponding to the individual trimmed states in the series of states used to represent the transitional flight. ASPAID requires the following user-specified information:

1. The number of trimmed states a vehicle rotor passes through during a transitional flight. Each trimmed state corresponds to a separate waypoint.

2. The beginning of each waypoint, specified as the number of rotor revolutions from the start of the flight. The vehicle starts in the first trimmed state. As an example, if the script specifies the second and third trimmed states as starting at two and 10 revolutions, respectively, there are eight rotor revolutions in the transition from the second to third trimmed state.

ASPAID performs linear interpolation over the contents of the blade data files through all the waypoints/trimmed states. The interpolated data are written by ASPAID as aperiodic blade data files containing the blade loading, motion, and geometry for transitional flight for all blades. The duration of flight trajectories between trimmed states must be represented as integer multiples of a rotor rotation period in the current ASPAID implementation.

The output of the ASPAID tool is used as input to the NAF F1A Synthesis Plugin. The plugin treats the ASPAID output as it does data for single flight conditions. Therefore, the F1A Synthesis Plugin developed in Ref. [12] is already capable of using the ASPAID output.

Section 4.2 describes a test of transitional flight tonal synthesis with the ASPAID/NAF combination.

3. Self Noise for Transitional Flight

3.1 Existing Self Noise Synthesis Methods

Audible broadband self noise is synthesized starting with numerical predictions for the self noise. Examples of these predictions for two emission angles are shown in Figure 1. Each point on a discretized source noise hemisphere surrounding a vehicle rotor corresponds to a different emission angle. Each discrete emission angle point contains a unique self noise prediction. The numerical self noise prediction is in the form of a one-third octave band (OTOB) spectrogram over a single rotor rotation period. Modulations in the sound pressure level (SPL) over the rotor rotation period result in peaks that repeat at a rate proportional to the rotor blade passage frequency.
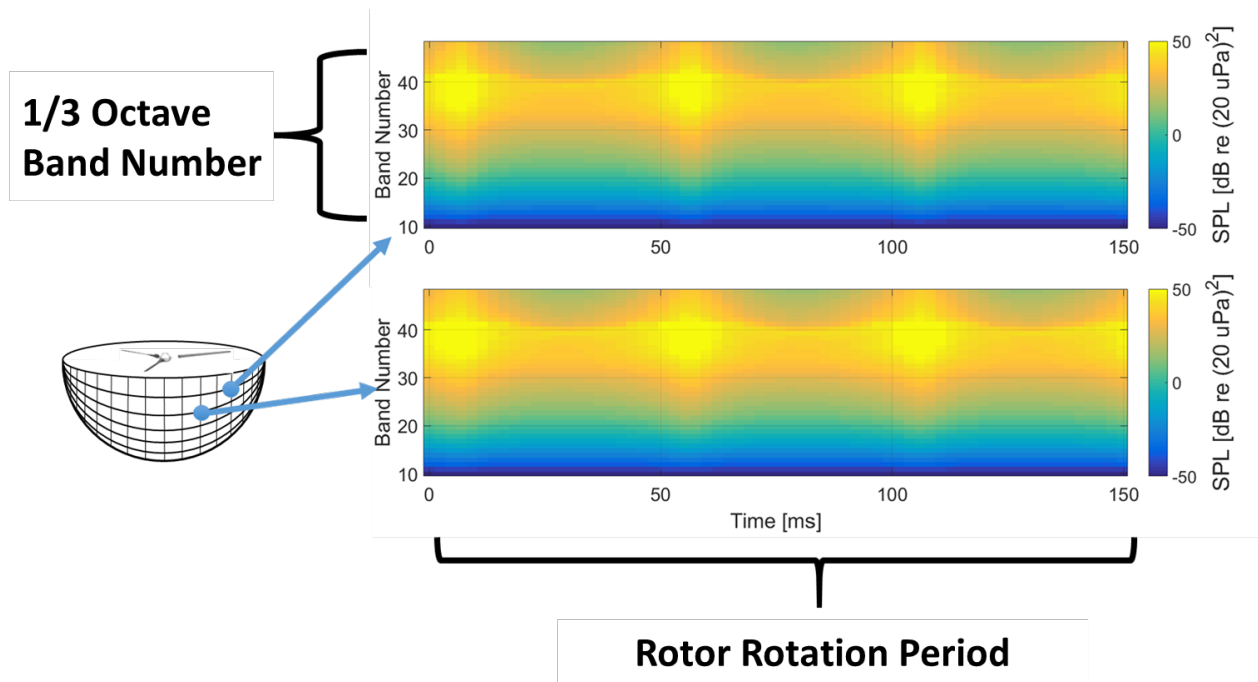

Figure 1: Self noise acoustic predictions on rotor source noise hemisphere.

The self noise hemispheres are predicted in this work using the ANOPP2 Self Noise Internal Functional Module (ASNIFM). That module uses the Brooks, Pope, and Marcolini self noise model [16] in a rotating frame, which combines computational and empirical analyses to compute self noise from the trailing edge of a rotor blade using frequency domain data. ASNIFM uses rotor blade effective angle of attack and blade inflow velocity data provided by CAMRAD II. Since CAMRAD II produces rotor blade data for individual vehicle trimmed states, the self noise hemispheres around individual vehicle rotors correspond to single flight conditions and not to transitional flight.

Multiple tools exist to synthesize self noise predictions into audible sound. For example, the NAF Modulated Broadband Synthesis Plugin modulates stochastic signals by self noise acoustic predictions through a series of steps described in Ref. [17]. These steps impart random phase to magnitude-only predictions to synthesize audible self noise inclusive of OTOB SPL modulations. The plugin uses source noise hemisphere data over the multiple emission angles traced by the rotor flyover of a ground observer. A different tool to synthesize self noise is given in Ref. [18], where the predicted OTOB spectrograms are converted into narrowband magnitude-only spectrums. Starting from an initial estimate signal, Ref. [18] uses the Griffin-Lim [19] algorithm to iteratively estimate a signal inclusive of phase but with spectral magnitude close to the self noise predictions. For transitional flight self noise synthesis, both tools need representative self noise acoustic predictions.

The approach in Ref. [18] may provide self noise predictions over changing rotor rotation speeds, but the rotor blade data is of insufficient fidelity from methods meant for real-time sound synthesis. When tools like ASNIFM generate separate self noise hemispheres for each trimmed state from higher fidelity blade data than can be produced in real-time, a method to combine the separate acoustic predictions for the different trimmed states is needed.

3.2   Combining Self Noise Acoustic Predictions from Multiple Trimmed States

This section describes the self noise synthesis method that has been developed for transitional flight when there is a separate acoustic prediction for each of the constituent trimmed states. Previously, when developing the NAF Modulated Broadband Synthesis Plugin, self noise sound pressure levels at different emission angles on a source noise hemisphere for a single trimmed state were interpolated over the emission angles spanning the simulated flight over a stationary ground observer [17]. This same interpolation process has now been extended to multiple source noise hemispheres in addition to multiple emission angles. Each source noise hemisphere corresponds to a different trimmed state that a vehicle is approximated to move through during transitional flight.

In self noise synthesis of a rotor flyover, emission angles as a function of time from rotor to ground observer are first found from the vehicle trajectory and the ground observer position. Figure 2 illustrates the determination of emission angles using an exaggerated discretization of source noise hemispheres around rotors. First, the emission angles at three consecutive time samples, t_A, t_B, and t_C, are found. In this example, the azimuth emission angle, ϕ, remains constant, but the elevation emission angles, θ_A, θ_B, and θ_C, change at time samples t_A, t_B, and t_C, respectively. The emission angles are a function of time in the bottom right plot in Figure 2.
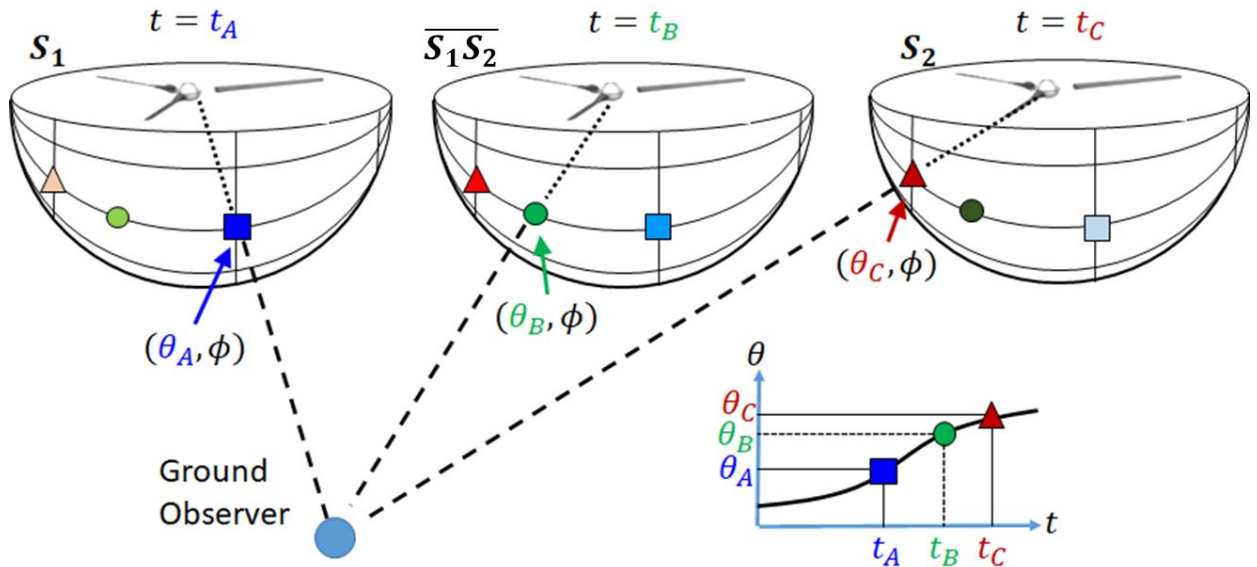

Figure 2: Changing emission angles during rotor flyover.

Figure 2 is like the illustration given in Ref. [15] to describe the self noise synthesis method. A difference from Ref. [15] is that the source noise hemispheres in Figure 2 do not represent the same flight condition. At time t_A, the source noise hemisphere gives self noise predictions for Trimmed State S_1. At time t_C, the source noise hemisphere gives self noise predictions for Trimmed State S_2. At times t_A and t_C, the emission angles correspond to prediction points on the respective source noise hemispheres, represented by the dark blue square and dark red triangle, respectively.

6

At time t_B, the emission angle falls on a point, represented by the green circle, that is between prediction points and between trimmed states. The source noise hemisphere, $\overline{(S_1 S_2)}$, at time t_B is formed by interpolating the self noise OTOB predictions between the OTOB predictions of the S_1 and S_2 source noise hemispheres. OTOB values at the red triangle and blue square for $\overline{(S_1 S_2)}$ are found from a weighted average, i.e., interpolation, of the predictions at both the triangles and the circles, respectively, from both S_1 and S_2. Data for the green circle at time t_B is found from a weighted average of the data at the triangle and square at time t_B.

After interpolating OTOB data between trimmed states, the self noise synthesis method proceeds the same way as that described in Ref. [15] for single flight conditions/trimmed states. Reference [15] details how the OTOB data are interpolated for the self noise synthesis method.

Section 4.3 tests the transitional flight self noise synthesis approach.

3.3   NAF Implementation

The NAF Modulated Broadband Synthesis Plugin [17] has been updated to implement transitional flight self noise synthesis. It is updated to accept multiple source noise hemispheres for each vehicle rotor, with each hemisphere representing a different trimmed state for the transitional flight. The NAF Plugin uses the weighted average approach described in Section 3.2 for interpolating self noise predictions across emission angles and prediction hemispheres. The NAF allows a user to specify the start times of each trimmed state, which define the waypoints of the flight. The updated NAF Modulated Broadband Synthesis Plugin is currently being tested for quality assurance before being included in a future release of the NAF. Transitional flight results from the plugin will be presented in future work. Results in this paper utilize a prototype program for transitional flight self noise synthesis.

4.   Testing Transitional Flight Noise Synthesis

4.1   Testing Strategy

Transitional flight synthesis testing occurred separately for tonal noise and self noise synthesis. Section 4.2 describes testing the synthesized sound with only the tonal noise being produced. Section 4.3 describes testing with only the synthesized self noise produced. Both sections refer to the same testing strategy that will be described in this current section (Section 4.1). Both the tonal noise and self noise syntheses tests use a single rotor in transitional flight. Using a single rotor for testing simplifies analyses with a SPL of the synthesized sound that is computed every rotor rotation period. There are three objectives for testing tonal noise and self noise transitional flight synthesis methods, where the objective depends on the flight conditions.

When flight conditions are constant, Test Objective 1 applies, and involves a comparison of results from the transitional flight synthesis methods with results from previous synthesis methods for steady flight.

Test Objective 2 applies when there are different trimmed states within a single flight. This objective verifies that the synthesized results obtained at the different trimmed states do not produce aberrant behavior where the flight condition is constant within a transitional flight. Aberrant behavior could potentially arise from incorrect implementation in specifying trimmed states.

Test Objective 3 applies to time intervals when the flight conditions are transitioning between trimmed states. The transitional flight sound that is synthesized between the different

trimmed states is compared with another synthesized sound that is produced when an intermediate trimmed state is specified between the two states.

Table 1 lists the hypothetical flight profiles created to meet the above three test objectives. Each row represents a flight profile consisting of two to five waypoints, t_1 to t_5. The trimmed state at a waypoint time t_k is identified as S_k. The transition between trimmed states occurs between waypoint start times. An arrow in the table represents a transition between the adjoining trimmed states. The four flight profiles are different only in the trimmed states that begin at each waypoint.

Table 1: Transitional flight noise synthesis test matrix.

		Waypoint Start Times				
		t_1	t_2	t_3	t_4	t_5
Flight Numbers	Flight 1	S_1	→	→	→	S_1
	Flight 2	S_2	→	→	→	S_2
	Flight 3	S_1	S_1	S_3	S_2	S_2
	Flight 4	S_1	S_1	→	S_2	S_2

Flights 1 and 2 start and end in Trimmed states S_1 and S_2, respectively. These two flights are synthesized with existing methods for constant flight conditions as performed in Refs. [12, 15, 17]. The results are used as benchmarks for comparing with results generated using the new synthesis methods applied to Flights 3 and 4 for tonal and self noise transitional flight.

Flight 3 uses the new synthesis methods for its entirety, from time t_1 to time t_5. This flight transitions from S_1 to S_2 through an intermediate state S_3, where S_3 is chosen from the available state database as a reasonable intermediate state between S_1 and S_2. The synthesis results at the beginning of Flight 3 can be compared with results from Flight 1, and results at the end of Flight 3 can be compared with the results from Flight 2. Comparing synthesis results from Flight 3 with results from Flights 1 and 2 will satisfy the first two test objectives.

Metrics for the comparisons are the SPL time histories of the flight profiles with samples computed every rotor rotation period. From t_1 to t_2, the SPLs of the synthesized sounds for Flights 1 and 3 should match. From t_4 to t_5, the SPLs of the synthesized sounds for Flights 2 and 3 should match. For the SPL comparisons between Flights 1, 2, and 3, a threshold for determining a good match was established based on visual inspection of the SPL time histories. For the results in this paper, a good match occurs if there is a difference of less than 0.1 dB between the SPL time histories of Flights 1, 2, and 3.

Flight 4 is similar to Flight 3 but transitions from S_1 to S_2 without going through trimmed state S_3. In Flight 4, the intermediate state between S_1 and S_2 is determined by the interpolation method, so this flight provides an opportunity to meet Test Objective 3 by comparing the interpolated state at time t_3 with the specified state S_3 from Flight 3.

Comparing Flights 3 and 4 will also use their SPL time histories that are computed every rotor rotation period. Unlike for the SPL time history comparisons between Flights 1, 2, and 3, the threshold for determining a good match between the SPL values for Flights 3 and 4 will be based on the Just Noticeable Difference (JND) for SPL. The SPL JND measures the SPL difference above which two sounds become audibly distinguishable to a listener. In Ref. [20], for 1 kHz tones with loudness levels of at least 60 Phons, the JND for SPL appears

to be at or slightly above 0.5 dB.[1] From the SPL time histories of Flights 3 and 4, the SPL difference at time t_3 will be compared with the SPL JND of 0.5 dB.

Trimmed state S_3 was selected from a database of available trimmed states as being a good approximation of the rotor state during the transition. However, limitations of the state database mean S_3 may not necessarily represent the true rotor characteristics at time t_3 if the vehicle were transitioning between states S_1 and S_2. Nonetheless, S_3 was chosen as the best available representation in the database of the transitional flight at the intermediate waypoint. Due to this possible mismatch between the state from the database and the interpolated rotor characteristics, the existence of an SPL difference up to 0.5 dB between Flights 3 and 4 at time t_3 is acceptable.

Tonal and self noise sounds for all four flights are synthesized at an observer, and the emission angle from rotor to observer changes with time. In all four flights, the observer maintains a constant distance from the rotor because propagation effects to a ground observer are not yet applied during sound synthesis. The emission angle time history is generated from the rotor flight path. The flight path may be specified using airspeeds and climb angles from trimmed states. However, the flight simulations allow for different airspeeds and climb angles from those that characterize the trimmed states.   In addition to having common trimmed states, Flights 1 and 2 required the same rotor-to-observer emission angle as Flight 3 to meet Test Objectives 1 and 2. Flights 3 and 4 required the same rotor-to-observer emission angles to meet Test Objective 3. Therefore, all four flights were forced to have identical emission angles regardless of their trimmed states.

The rotor that will be used for transitional flight synthesis testing in this paper is a single three-bladed rotor from the six-passenger NASA UAM Quadrotor Reference Vehicle [21], shown in Figure 3. The vehicle uses collective control due to the large radius (13.10 ft (3.99 m)) of the rotors. The rotor rotation speed is 400.92 revolutions per minute (RPM) giving a blade passage frequency of approximately 20 Hz and a rotor rotation period of 150 ms. All synthesized sounds, both tonal and self noise, are generated 100 meters away from the rotor without applying propagation effects. For the synthesized tonal noise, an additional processing step scales the sounds by 0.07 so they can be played over computer speakers without clipping.

Figure 3: NASA UAM Quadrotor Reference Vehicle.

The test matrix in Table 1 helps verify that the simulated sounds are being generated as intended, but it does not validate the synthesis approaches. Validation of the synthesis

---

[1] Reference [20] based its results on 1 kHz tones and not rotorcraft sounds. There does not appear to be research available on JND to rotorcraft sounds in the literature. Rotorcraft tonal noise consists of tones at multiple frequencies. Rotor broadband self noise contains modulations by a tonal signal. Due to these rotorcraft noise characteristics, this current paper assumes that the SPL JND from Ref. [20] applies to the SPL JND for both tonal and broadband self noise from a UAM vehicle rotor.

approaches requires data from flight tests with real aircraft, data from wind tunnel measurements, or predicted data that have been verified as being accurate. Such data are not presented in this paper.

4.2   Testing Synthesis of Loading and Thickness Noise for Transitional Flight

Testing the use of ASPAID for transitional flight loading and thickness, i.e., tonal, sound synthesis through the NAF F1A Synthesis Plugin follows the test matrix from Table 1. The trimmed states used in the testing all have a constant climb angle of positive 5 degrees but have different airspeeds. These trimmed states were selected because they help test a transitional flight approximating an accelerated climb. Trimmed states S_1 and S_2 have airspeeds of 40 KTAS and 60 KTAS, respectively. Intermediate trimmed state S_3 has an airspeed of 50 KTAS.

To be consistent with ASPAID data, waypoint times were adjusted to be multiples of the rotor rotation period (150 ms). Corresponding to Table 1, $t_1 = 0$ s, t_2 occurs at 10 rotor revolutions (~1.5 s), t_3 occurs at 40 rotor revolutions (~6 s), t_4 occurs at 70 rotor revolutions (~10.5 s), and t_5 occurs at 80 rotor revolutions (~12 s).

Figure 4 compares the SPL time histories of single Quadrotor rotor tonal sounds of the four synthesized flights from Table 1. Waypoint times are indicated by the vertical dashed traces. The elevation and azimuth emission angle time histories in Figure 4 are from rotor to observer. Flights 1 (red) and 2 (blue), represented by dotted traces, have constant airspeeds of 40 and 60 KTAS, respectively. The tonal noise for Flights 1 and 2 was synthesized with data directly from CAMRAD II as is done with existing methods [12]. Flights 3 (dotted black trace) and 4 (solid black trace) have variable airspeeds and were synthesized using ASPAID data. Within these two flights, trimmed states S_1, S_2, and S_3 are each given a different color for the vertical dashed lines that represent their start times. Shaded areas in red and blue represent where the trimmed state, and hence the airspeed, is constant for Flights 3 and 4. Time history audio files corresponding to the four flight profiles are available for listening in Ref. [22].
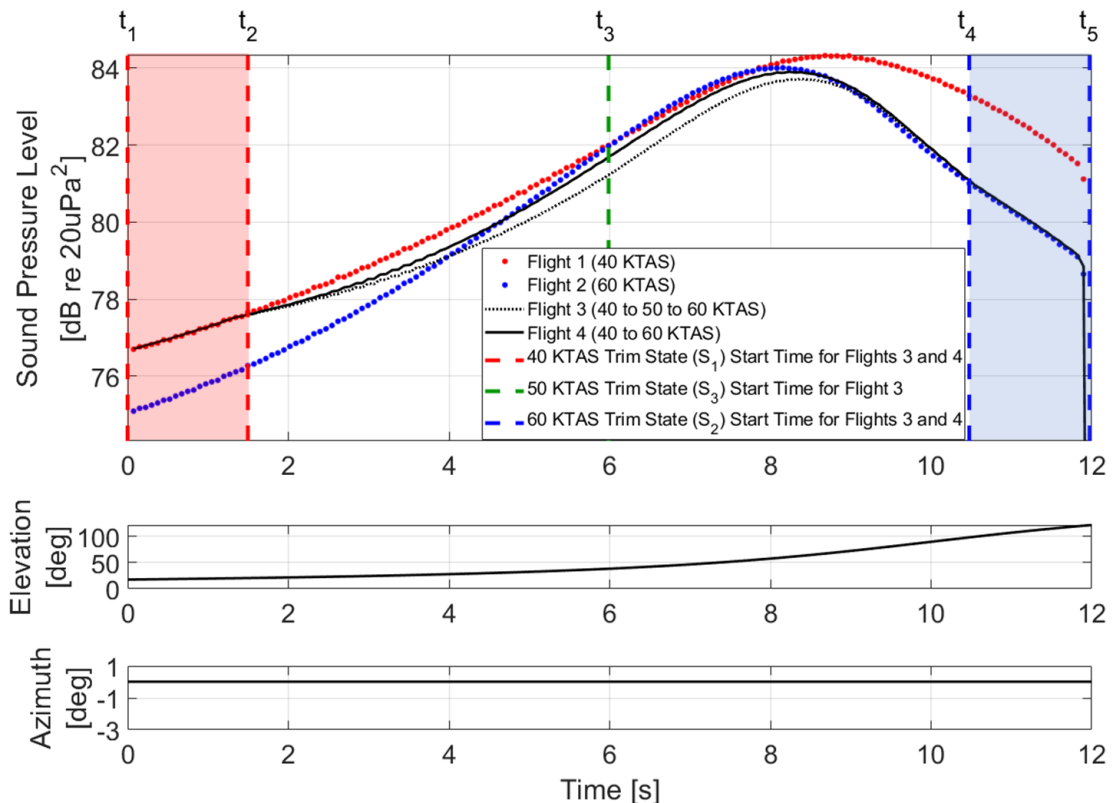

Figure 4: Testing loading and thickness noise transitional flight sound synthesis.

Figure 4 indicates that the transitional flight synthesis with ASPAID data produce intended results. Specifically, the synthesized sound SPL of Flight 3 matches Flight 1 between waypoints t_1 and t_2 with the SPL difference between the flights at each time sample being less than 0.1 dB. Flight 3 also matches Flight 2 between waypoints t_4 and t_5 with the SPL difference between the flights at each time sample being less than 0.1 dB. Hence, Test Objectives 1 and 2 are met for transitional flight tonal noise synthesis. There is a 0.5 dB difference between Flights 3 and 4 at time t_3 when Flight 3 reaches S_3. The sounds in Figure 4 have loudness levels (not shown) between 65 Phons and 75 Phons. The SPL JND of 0.5dB from Ref. [20] applies to tones with loudness levels of at least 60 Phons. Therefore, Flights 3 and 4 having a SPL difference of 0.5 dB appears to indicate that they are perceptually similar, which meets Test Objective 3 for transitional flight tonal noise synthesis. Other trimmed state combinations were tested, and the results are consistent with those shown in Figure 4.

4.3 Testing Synthesis of Self Noise for Transitional Flight

Different combinations of three trimmed states were tested for the self noise synthesis, and the results from one set of trimmed states are shown in this paper. Like the trimmed states used to test tonal noise synthesis in Figure 4, the states for transitional flight self noise synthesis testing were selected to approximate vehicle acceleration. However, the three trimmed states to test self noise synthesis have different airspeeds (60 KTAS, 70 KTAS, and 80 KTAS) from those used to test tonal noise synthesis, and they all represent level cruise conditions. All trimmed state data came from CAMRAD II, and a source noise hemisphere for each of the trimmed states was generated for the Quadrotor rotor. Unlike for the tonal noise synthesis described in Section 2, ASPAID was not involved in the self noise synthesis. For that reason, waypoint times in testing were not adjusted to be multiples of the rotor rotation period.

Testing transitional flight self noise sound synthesis follows the test matrix from Table 1. Figure 5 compares the SPL time histories of synthesized self noise sounds from a single Quadrotor rotor for the four flight profiles from Table 1 using the three trimmed states. The Figure 5 legend gives airspeeds for S_1, S_2, and S_3. The Figure 5 elevation and azimuth emission angle time histories are from rotor to observer. Corresponding to Table 1 and the vertical dashed traces in Figure 5, the waypoints for the flight were $t_1 = 0$ s, $t_2 = 3$ s, $t_3 = 13$ s, $t_4 = 23$ s, and $t_5 = 26$ s. Flights 1 (red) and 2 (blue), represented by dotted traces, have a constant airspeed of 60 and 80 KTAS, respectively. Sounds for Flights 1 and 2 were synthesized using the existing self noise synthesis approach from Ref. [15] for constant flight conditions. Flight 3, which transits through all three trimmed states, is represented by the dotted black trace. The red vertical dashed traces represent the Flight 3 waypoints with S_1 (times t_1 and t_2). The green vertical dashed trace represents the Flight 3 waypoint with S_3 (time t_3). The blue vertical dashed traces represent the Flight 3 waypoints with S_2 (times t_4 and t_5). Flight 4, which is like Flight 3 but without S_3, is represented by the solid black trace. Shaded areas in red and blue represent where the trimmed state, and hence the airspeed, is constant for Flights 3 and 4. All four flight profiles are available for listening in Ref. [22].
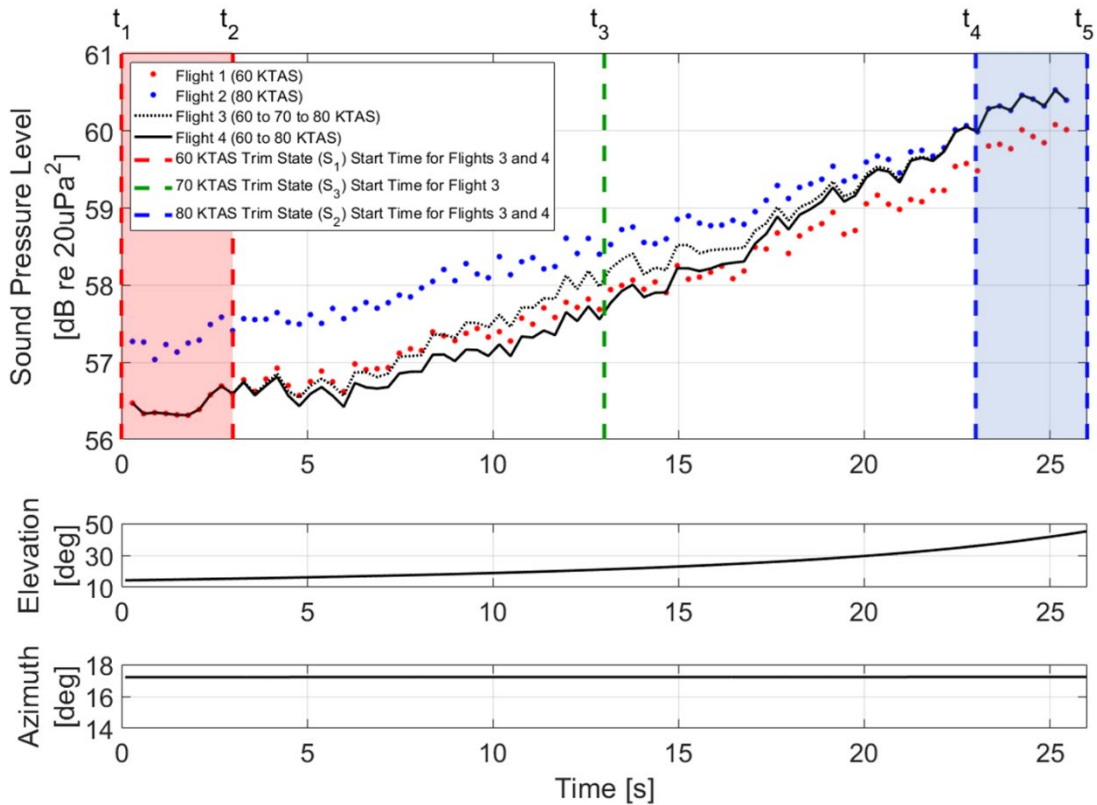
Figure 5: Validating self noise transitional flight sound synthesis.

The results from Figure 5 are similar to those obtained for tonal noise synthesis for transitional flight in Figure 4. Figure 5 indicates that self noise synthesis for transitional flight produces intended results. Flight 3 matches with Flight 1 between waypoints t_1 and t_2 with the SPL difference between the flights at each time sample being less than 0.1 dB. Flight 3 also matches with Flight 2 between waypoints t_4 and t_5 with the SPL difference between the flights at each time sample being less than 0.1 dB. Hence, Test Objectives 1 and 2 are met for transitional flight self noise synthesis. There is an approximately 0.4 dB difference between Flights 3 and 4 and time t_3 when Flight 3 is at S_3. Loudness levels (not shown) of Flights 3 and 4 are between 65 Phons and 80 Phons. Therefore, Flights 3 and 4 having an SPL difference of less than 0.5 dB at time t_3 appears to suggest that the sounds are perceptually similar, which meets Test Objective 3 for transitional flight self noise synthesis. For other trimmed state combinations that were tested, results were like that shown in Figure 5 but are not provided in this paper.

5. Auralization of Vehicle Flight Maneuvers

5.1 Background

In Ref. [23], the NASA UAM Quadrotor reference vehicle was simulated in transitional flight departure and approach maneuvers to generate contour maps of A-weighted Sound Exposure Level (SEL-A). A module called the ANOPP2 Mission Analysis Tool (AMAT) simulated the maneuvers using multiple trimmed states for the UAM vehicle. These maneuvers were also part of a simulated UAM flight route in the New York City metropolitan area that Ref. [24] analyzed for noise annoyance. AMAT used source noise hemispheres underneath the entire aircraft instead of underneath individual rotors. While this analysis resulted in noise predictions from the maneuvering vehicle, no acoustic pressure time history data were produced that could be presented as audible sound.

In this work, the same departure and approach maneuvers from Ref. [23] were auralized using the same series of vehicle trimmed states. The A-weighted SPL (SPL-A) time histories and SEL-A values at observers common to both AMAT simulations and the auralizations will be compared. The comparisons will offer evidence beyond the results from Section 4 that

the transitional flight sound synthesis approaches are producing intended results. The comparisons will not validate the auralization accuracy because the simulated sounds are being compared with another simulation. Unlike in Section 4, which auralized sound from a single rotor, sounds from all rotors of the Quadrotor are included in these departure and approach auralizations. The CAMRAD II trimmed state data used in Ref. [23] for the departure and approach maneuvers were available for each of the UAM Quadrotor rotors.

In this paper, comparisons with AMAT simulations are only shown for the self noise auralizations. Comparison of tonal noise auralizations with AMAT results revealed an unexplained discrepancy. The source of the discrepancy is not understood at this point, but it will be investigated in future work.

5.2 Departure Flight Auralization and Comparison with AMAT Result

Figure 6 shows the departure flight profile as defined in AMAT. Distances are approximately to scale. The aircraft flies along the black trace from left to right within the vertical plane, i.e., there is no lateral movement. The graph gives the vehicle position in ground range and altitude. The black "x" symbol on the horizontal axis at a ground distance of 0 [ft] is the observer, i.e., listener, with listening height of 4 [ft] above ground. The observer is along the flight centerline. Numbers that are encircled by ovals are the trimmed states/waypoints of the flight. The blue dashed vertical traces identify the location along the flight trajectory where each waypoint occurs. The separation between Trimmed States 1 and 2 is not visible in this figure.
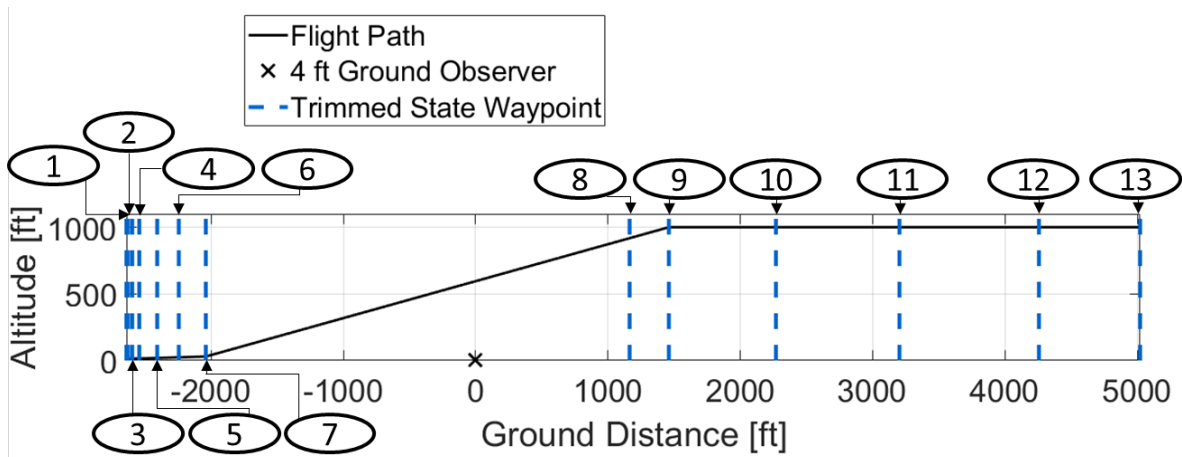

Figure 6: Departure flight profile with trimmed states numbered within ovals.

Table 2 also gives trimmed state start times that correspond to the vertical blue dashed traces from Figure 6. Although tonal noise auralizations are not shown for the departure and approach profiles in this paper, they are expected to be added in future work. Therefore, trimmed state start times in Table 2 are adjusted from the Ref. [23] AMAT simulation start times to be multiples of the rotor rotation period (150 ms), as required by ASPAID. A maximum offset of 150 ms in start times between waypoints in the AMAT simulations and auralizations is assumed to have negligible impact on SEL-A values.

Table 2 also gives the characteristics of the 13 trimmed states/waypoints from Figure 6. Each trimmed state is identified by an airspeed and climb angle. Each trimmed state also has an associated pitch angle of the vehicle (not shown) about the vehicle center of gravity. Vehicle roll angles were negligible for all trimmed states and are therefore set to zero degrees here. All trimmed states have the same rotor rotation speed of 400.92 RPM for all the Quadrotor rotors.

The simulated climb angle in Table 2 refers to the actual climb angle used in the departure flight trajectory. For states 2-8, the simulated climb angle is different from the trimmed state

climb angle. This difference is visible in Figure 6, where the black trace does not have a constant slope of five degrees between Trimmed States 2 and 8. Instead, the slope changes according to the simulated climb angles specified in Table 2. The difference between the trimmed state and simulated climb angles arises because Ref. [23] based the AMAT Quadrotor flight trajectory on an existing conventional helicopter flight profile. This helicopter flight profile had simulated climb angles that did not match climb angles of Quadrotor trimmed states in the available database. Therefore, Ref. [23] used the trimmed states in Table 2 for the departure profile based on the closest climb angle match in the available database of trimmed states.

Table 2: Departure profile trimmed states.

Trimmed State (TS) Number	1	2	3	4	5	6	7
TS Start Time [s]	0	1.35	2.59	3.89	6.14	8.38	10.5
TS Airspeed [KTAS]	0	10	20	30	40	50	60
TS Climb Angle [deg]	0	5	5	5	5	5	5
Simulated Climb Angle [deg]	0	0	0	1.7	1.7	1.7	15.5

Trimmed State (TS) Number	8	9	10	11	12	13	
TS Start Time [s]	42.1	45.0	52.5	59.9	67.2	72.3	
TS Airspeed [KTAS]	60	60	70	80	90	90	
TS Climb Angle [deg]	5	0	0	0	0	0	
Simulated Climb Angle [deg]	15.5	0	0	0	0	0	

The auralization results shown in this paper were performed with all rotors at the vehicle center of gravity. If the rotors were instead placed at their true center locations around the vehicle, they would each have a slight lateral offset from the flight trajectory in Figure 6. Near the beginning and end of the departure profile where the azimuth emission angle from the rotor to the ground observer changes rapidly, these slight lateral offsets cause artifacts in the simulated SPL-A time history. Future work will seek to eliminate these artifacts so that the rotors can be simulated at their true center locations.

AMAT simulations in Ref. [23] approximated the departure and approach flights with a constant flight condition between waypoints. The approximation was achieved by creating a 'guard' waypoint that duplicated the previous trimmed state, which was placed immediately before the next trimmed state [25]. Hence, in the AMAT simulations, a step-change in airspeed occurred just before the next trimmed state. Guard waypoints were not used for the auralizations in this paper, but instead the vehicle airspeed was allowed to continuously change between different trimmed states. The average segment airspeed was approximately the same between AMAT and the auralizations, so the segment durations were nearly the same, within the time of a single rotor rotation period. Nevertheless, the lack of guard waypoints in the auralizations did create differences between the AMAT and auralization results, with the deviation growing with the duration between trimmed states. For this reason, Trimmed State 8 in the departure profile is identical to state 7. It allows for the same flight condition to be maintained in the long 15.5 degree climb between states 7 and 8 to match the AMAT simulation.

Propagation parameters were identical between the AMAT simulation from Ref. [23] and the auralizations in this paper. Specifically, the atmospheric absorption model, SAE 866 [26], was used for both simulations, and atmospheric conditions corresponded to a uniform atmosphere at 15°C, 1 atm, and 70% relative humidity. Propagation effects for the auralizations were applied through the NAF. The effect of a soft ground was modeled using the Delany and Bazley single-parameter impedance model [27] with a flow resistivity of 250000 Rayls. Ground reflections were included in the auralizations with the listeners/observers receiving propagated sounds four feet above the ground. Both AMAT and the auralizations used spherical wave propagation and not plane wave propagation. At

shallow incidence angles, the spherical wave ground reflection computation is implemented differently in the NAF than in AMAT. Some deviation in AMAT and auralization results is expected when emission angles from the source cause shallow incidence angles at the observer.

Figure 7 shows the SPL-A self noise time histories from AMAT and transitional flight auralization of the NASA UAM Quadrotor at the ground observer for the departure profile. The numbered ovals refer to the trimmed states in Figure 6 and Table 2. The SPL-A time history for the auralization was computed after combining the auralized sounds from all four rotors. With all rotors being simulated as being at the vehicle center of gravity, the azimuth emission angle is zero degrees for all four rotors. The match between AMAT and the auralization is good until the elevation emission angle is larger than 155 degrees. There is also some mismatch when the emission angle is near zero degrees. Differences in the spherical wave ground reflection computation between AMAT and the NAF contribute to the mismatch.   When comparing the AMAT and auralization SPL-A time histories for an individual rotor (not shown), the deviation between the time histories is visually apparent when the elevation emission angle is greater than 160 degrees. The mismatch in Figure 7, which is noticeable earlier in time, is partly a cumulative result over all four rotors.   The SEL-A value for the AMAT result in Figure 7 is 70.9 dBA, and the SEL-A value for the auralization is 71.2 dBA. With the SEL-A difference being less than 0.5 dB, the two levels should be regarded as indistinguishable.
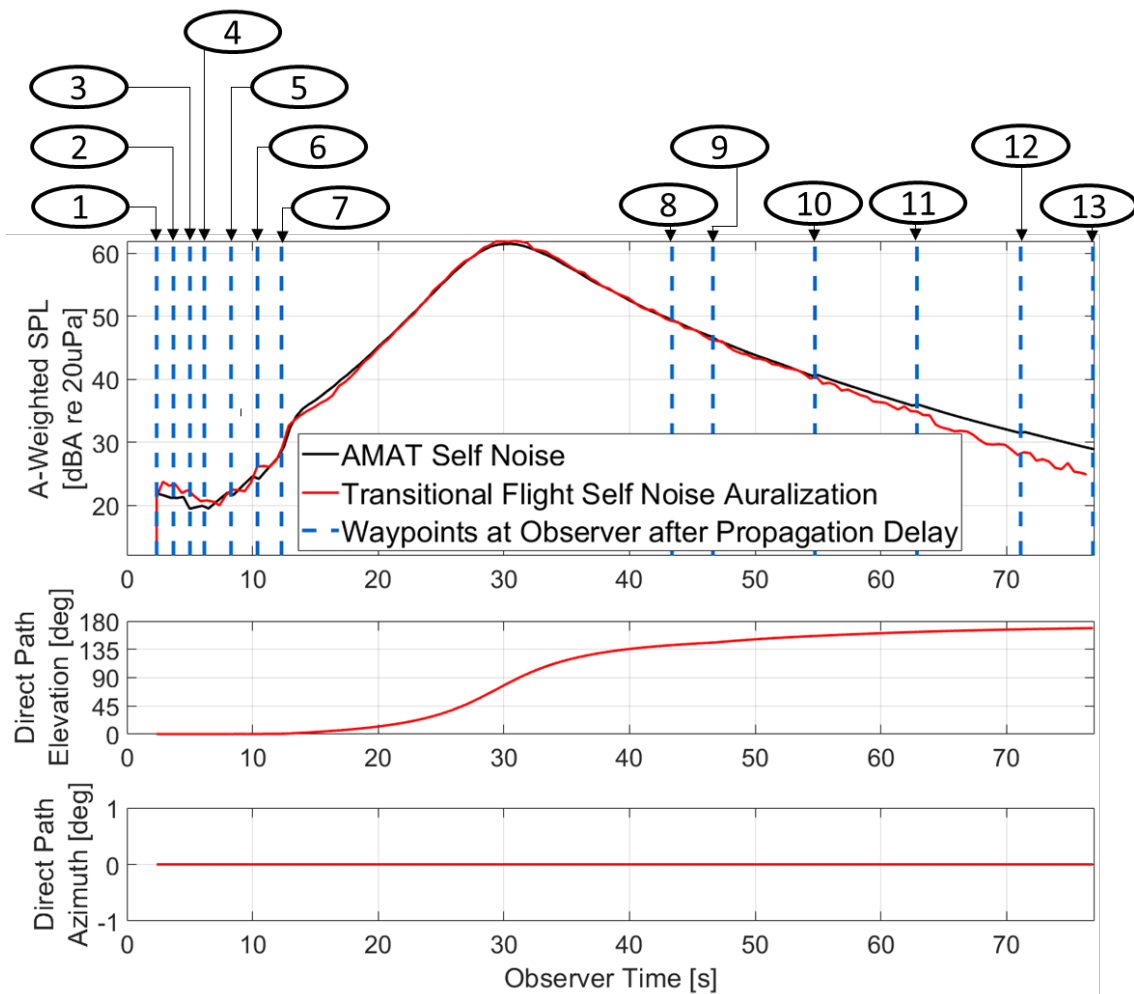

Figure 7. Comparing AMAT results and transitional flight auralization for departure.

The self noise auralization of the NASA UAM Quadrotor flying the departure maneuver, as heard by the Figure 6 observer, is available online [22]. When listening to the sound, Figure

6, Table 2, and Figure 7 may help to illustrate which trimmed states the vehicle is transitioning through.

5.3 Approach Flight Auralization and Comparison with AMAT Result

Figure 8 shows the approach flight profile as defined in AMAT in a format similar to Figure 6 of the previous section. As for the departure case, all rotors are positioned at the vehicle center of gravity, and there is no lateral movement. Here, the ground observer is also along the flight centerline and is four feet above the ground.
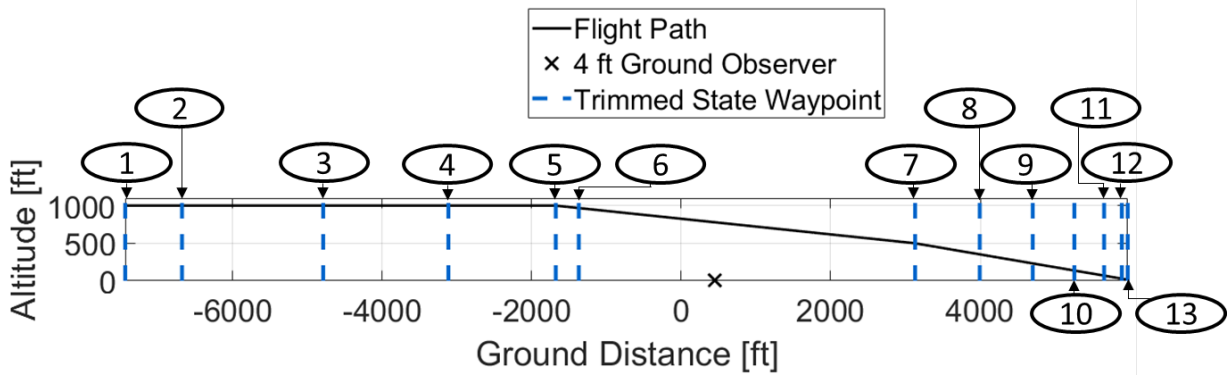

Figure 8: Approach flight profile with trimmed states numbered within ovals.

Table 3 identifies the 13 trimmed states/waypoints from Figure 8. Trimmed state start times for the approach profile are multiples of the rotor rotation period so that tonal noise from ASPAID data may later be included in the auralization. In the auralization, airspeed continually changes through the maneuver except in the long descent between states 6 and 7, which are the same trimmed states. As mentioned in the previous section (Section 5.2), the AMAT simulation in Ref. [23] maintained constant flight conditions between trimmed states by using guard waypoints. The constant flight condition between states 6 and 7 in the auralization was to reduce discrepancies with the AMAT results. The trimmed state and simulated climb angles reflect aircraft descent. See the previous section for a description of the difference between the trimmed state and simulated climb angles. As with the departure, all trimmed states had the same rotor rotation speed of 400.92 RPM for all the Quadrotor rotors.

Table 3: Approach profile trimmed states.

Trimmed State (TS) Number	1	2	3	4	5	6	7
TS Start Time [s]	0	4.94	18.1	32.3	44.4	47.4	91.9
TS Airspeed [KTAS]	90	90	80	70	60	60	60
TS Climb Angle [deg]	0	0	0	0	0	-5	-5
Simulated Climb Angle [deg]	0	0	0	0	0	-5.9	-5.9

Trimmed State (TS) Number	8	9	10	11	12	13
TS Start Time [s]	101	111	120	129	139	146
TS Airspeed [KTAS]	50	40	30	20	10	0
TS Climb Angle [deg]	-5	-10	-10	-10	-20	0
Simulated Climb Angle [deg]	-9.7	-9.7	-9.7	-9.7	-9.7	-9.7

Figure 9 shows the SPL-A self noise time histories from AMAT and transitional flight auralization of the NASA UAM Quadrotor at the ground observer for the approach profile. The numbered ovals refer to the trimmed states in Figure 8 and Table 3. Propagation effects in the approach auralizations were the same as described for departure in Section 5.2 and match the propagation parameters in the Ref. [23] AMAT simulations. The SPL-A time history for the auralization was computed after combining the auralized sounds from all four rotors. With all rotors being simulated as being at the vehicle center of gravity, the azimuth emission angle is zero degrees for all four rotors. The match between AMAT and the

auralization is good until the elevation emission angle is larger than 160 degrees. A difference in spherical wave ground reflection computation between AMAT and the NAF and the cumulative effect of these differences over all four rotors contribute to the mismatch. Despite the mismatch near the end of the flight, the AMAT and auralization values of SEL-A in Figure 9 match within 0.04 dB, which is effectively an indistinguishable difference.
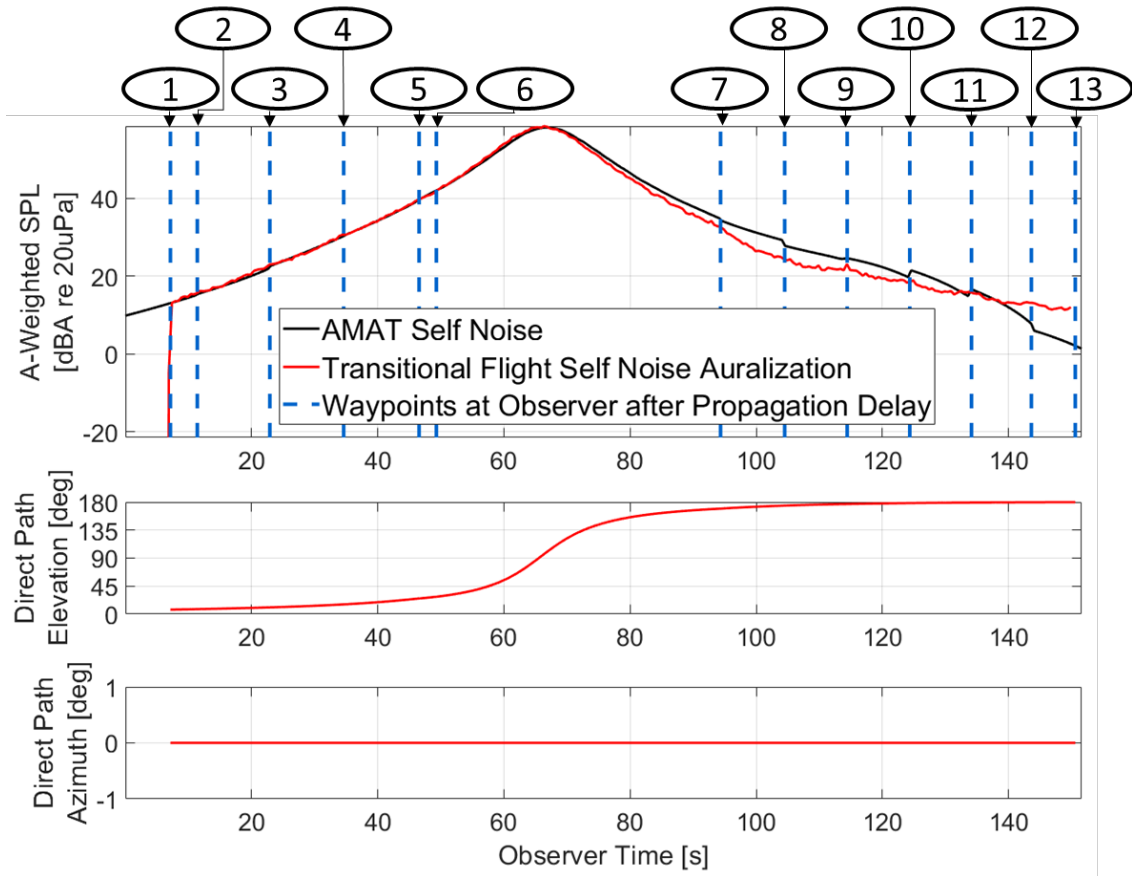

Figure 9. Comparing AMAT results and transitional flight auralization for approach.

The auralized self noise sound for the Quadrotor flying the approach maneuver may be listened to online at Ref. [22]. When listening to the sounds, Figure 8, Table 3, and Figure 9 may help to illustrate which trimmed states the vehicle is transitioning through.

6. Conclusion

This paper describes the development of approaches to synthesize rotor/propeller loading and thickness noise and broadband self noise for transitional flight when flight state data for the noise sources exist separately for different trimmed states. Transitional flight was approximated as a series of trimmed states with the vehicle smoothly transitioning from one state to another over a specified time interval. As part of this work, the ASPAID module was developed in ANOPP2 to combine blade loading, motion, and geometry data from a series of separate trimmed flight states into aperiodic data representing transitional flight. The ASPAID-generated data is formatted to be compatible with sound synthesis tools, like the NAF F1A Synthesis Plugin, to produce tonal noise for transitional flight auralizations. This work also extended an existing self noise synthesis method to use acoustic predictions from multiple source noise hemispheres, each representing a unique trimmed state, to synthesize self noise for transitional flight.

The tonal noise and self noise synthesis approaches for transitional flight were tested using a set of flight profiles with combinations of different trimmed states. For the trimmed states used, test results showed that the synthesis approaches operate as intended.

The self noise synthesis approach for transitional flight was exercised to auralize departure and approach flights of a UAM vehicle. The flights consisted of a series of separate vehicle trimmed states at specified waypoints. SPL-A and SEL-A values of the auralized sounds were compared to values generated from previous simulations where audible sounds were not produced. These comparisons demonstrated good agreement between the auralized SPL-A and SEL-A values and the previously simulated SEL-A values. The close comparisons demonstrate that the transitional flight self noise synthesis approach is operating as intended.

Validation of the transitional flight tonal and self noise synthesis approaches presented in this paper will require more extensive comparisons of the simulated sounds with flight measurements or with higher-fidelity predictions that are verified as being accurate.

Anticipated future work includes:

1. Complete the testing of the NAF Modulated Broadband Synthesis Plugin to implement transitional flight self noise synthesis.

2. Explain and eliminate the discrepancy between AMAT results and auralizations for transitional flight tonal noise. It will allow the departure and approach profile auralizations to have both tonal and broadband noise.

3. Eliminate artifacts when the azimuth emission angle from the rotor to the ground observer changes rapidly. Resolution of this issue will allow rotors to be auralized from their true center positions around the vehicle and not be co-located at the vehicle center of gravity.

REFERENCES

[1] M. Vorländer, Auralization - Fundamentals of Acoustics, Modelling, Simulation, Algorithms and Acoustic Virtual Reality, Springer-Verlag Berlin Heidelberg, 2008.

[2] S. A. Rizzi and A. K. Sahai, "Auralization of air vehicle noise for community noise assessment," *CEAS Aeronautical Journal,* vol. 10, pp. 313-334, 3 2019.

[3] S. A. Rizzi, D. L. Huff, D. D. Boyd, Jr., P. Bent, B. S. Henderson, K. A. Pascioni, D. C. Sargent, D. L. Josephson, M. Marsan, H. He and R. Snider, "Urban Air Mobility Noise: Current Practice, Gaps, and Recommendations," *NASA/TP–2020-5007433,* October 2020.

[4] C. E. Tinney, J. A. Valdez and Y. Zhao, "A Moving Source Model for Rotor Broadband Noise," in *AIAA AVIATION Forum, AIAA 2023-3222*, San Diego, CA, USA, 2023, https://doi.org/10.2514/6.2023-3222.

[5] N. A. Pettingill and N. S. Zawodny, "Identification and Prediction of Broadband Noise for a Small Quadcopter," in *Proceedings of the 75th Annual Forum, Paper 153*, Philadelphia, PA, USA, 2019.

[6] J. Ko, J. Jeong, H. Cho and S. Lee, "Real-time prediction framework for frequency-modulated multirotor noise," *Physics of Fluids,* vol. 34, no. 2, p. 027103, 2022.

[7] E. Greenwood, F. H. Schmitz and R. D. Sickenberger, "A Semiempirical Noise Modeling Method for Helicopter Maneuvering Flight Operations," *Journal of the American Helicopter Society,* vol. 60, no. 2, pp. 1-13, 2015.

[8] W. Johnson, "Comprehensive Analytical Rotorcraft Model of Rotorcraft Aerodynamics and Dynamics, Version 4.10," in *Johnson Aeronautics, Volumes I-9*, 2017.

[9] L. V. Lopes and C. L. Burley, "ANOPP2 User's Manual," NASA/TM-2016-219342, Hampton, VA, 2016.

[10] A. R. Aumann, B. C. Tuttle, W. L. Chapin and S. A. Rizzi, "The NASA Auralization Framework and plugin architecture," in *InterNoise 2015*, San Francisco, CA, USA, 2015.

[11] F. Farassat and G. P. Succi, "The Prediction of Helicopter Rotor Discrete Frequency Noise," *Vertica,* vol. 7, pp. 309-320, 1983.

[12] S. Krishnamurthy, B. C. Tuttle and S. A. Rizzi, "A Synthesis Plug-in for Steady and Unsteady Loading and Thickness Noise Auralization," in *AIAA AVIATION Forum, AIAA 2020-2597*, Virtual Event, 2020, https://doi.org/10.2514/6.2020-2597.

[13] L. V. Lopes, "ANOPP2's Farassat's Formulations Internal Functional Module (AFFIFMs) Reference Manual, Version 1.4," NASA-TM-20210021111, NASA Langley Research Center, Hampton, VA 23681, 2021.

[14] S. Krishnamurthy, B. C. Tuttle and S. A. Rizzi, "Auralization of Unsteady Rotor Noise using a Solution to the Ffowcs Williams- Hawkings Equation," in *Proceedings of the 75th Annual Forum, Vertical Flight Society*, Philadelphia, 2019.

[15] S. Krishnamurthy, S. A. Rizzi, R. Cheng and D. D. Boyd, Jr., "Prediction-Based Auralization of a Multirotor Urban Air Mobility Vehicle," in *AIAA SciTech Forum, AIAA 2021-0587*, Virtual Event, 2021, https://doi.org/10.2514/6.2021-0587.

[16] T. F. Brook and S. D. Pope, "Airfoil self-noise and prediction," NASA-RP-1218, Hampton, VA, 1989.

[17] S. Krishnamurthy, A. R. Aumann and S. A. Rizzi, "A Synthesis Plugin for Auralization of Rotor Self Noise," in *AIAA Aviation 2021 Forum, AIAA 2021-2211*, Virtual Event, 2021. https://doi.org/10.2514/6.2021-2211.

[18] J. Ko, Y. Kim, J. Jeong and S. Lee, "Prediction-based psychoacoustic analysis of multirotor noise under gusty wind conditions," *The Journal of the Acoustical Society of America,* vol. 154, no. 5, pp. 3004-3018, 2023.

[19] D. Griffin and L. Jae, "Signal estimation from modified short-time Fourier transform," *IEEE Transactions on Acoustics, Speech, and Signal Processing,* vol. 32, no. 2, pp. 236-243, 1984.

[20] J. H. Johnson, C. W. Turner, J. J. Zwislocki and R. H. Margolis, "Just noticeable differences for intensity and their relation to loudness," *The Journal of the Acoustical Society of America,* vol. 93, no. 2, pp. 983-991, 1993.

[21] C. Silva, W. R. Johnson, E. Solis, M. D. Patterson and K. R. Antcliff, "VTOL Urban Air Mobility Concept Vehicles for Technology Development," in *2018 Aviation Technology, Integration, and Operations Conference*, Atlanta, GA, 2018. doi: 10.2514/6.2018-3847.

[22] "Aircraft flyover simulation," NASA, 2024. [Online]. Available: https://stabserv.larc.nasa.gov/flyover/.

[23] S. J. Letica and S. A. Rizzi, "On the modeling of urban air mobility vehicle takeoff and landing operations in the FAA Aviation Environmental Design Tool," in *INCE NOISE-CON 2024*, New Orleans, LA, 2024.

[24] S. A. Rizzi, A. W. Christian, S. J. Letica and S. V. Lympany, "Annoyance Model Assessments of Urban Air Mobility Vehicle Operations," in *CEAS/AIAA Aeroacoustics 2024, AIAA 2024-3014*, Rome, Italy, 2024, https://doi.org/10.2514/6.2024-3014.

[25] S. A. Rizzi and R. Menachem, "Community noise assessment of urban air mobility vehicle operations using the FAA Aviation Environmental Design Tool," in *InterNoise 2021, Paper IN-2021-1482*, Virtual Meeting, 2021, https://doi.org/10.3397/IN-2021-1482.

[26] SAE International Recommended Practice, "Standard Values of Atmospheric Absorption as a Function of Temperature and Humidity for use in Evaluating Aircraft Flyover Noise," SAE Standard ARP866, 1964.

[27] M. E. Delany and E. N. Bazley, "Acoustical properties of fibrous absorbent materials," *Applied Acoustics,* vol. 3, no. 2, pp. 105 - 116, 1970.

[28] A. Christian, D. Boyd, Jr., N. S. Zawodny and S. A. Rizzi, "Auralization of tonal rotor noise components of a quadcopter flyover," in *InterNoise 2015*, San Francisco, CA, USA, 2015.